



Moment Curvature Analysis of Wide-Flange Steel Columns with Local Buckling Failure Mode

A. Niroomandi,

Aurecon, Auckland, New Zealand.

Gh. Hatef, M.A. Najafgholipour

Department of Civil and Environmental Engineering, Shiraz University of Technology, Iran.

ABSTRACT

This study examines the use of plastic hinge analysis to estimate the displacement capacity of wide flange steel columns in moment resisting frames. Initially, the accuracy of existing equivalent plastic hinge length formulas was evaluated by comparing analytical results against experimental data from 33 steel columns. The compressive stress-strain curve of steel was determined using the Kolwankar et al. (2020) method. Moment-curvature analysis was then conducted using SAP2000 software (2019). Our findings indicate that current formulas do not accurately estimate the displacement capacity of steel columns. Consequently, a new formula is proposed for determining the equivalent plastic hinge length, derived from a comprehensive numerical parametric study. This study was conducted using a rigorously validated finite element (FE) modelling approach in Abaqus software. The proposed formula shows promise for accurately estimating drift capacity of steel columns where local buckling is the primary mode of failure.

1 INTRODUCTION

Steel moment-resisting frames (MRFs) are widely used in buildings of varying heights and functions due to their structural efficiency. The key components of steel MRFs include beams, columns, and beam-to-column connections, each playing a critical role in the overall frame performance. Notably, columns are instrumental in ensuring the global stability of these structures. To prevent early instability in these critical elements, design and assessment codes focus on their robustness. Consequently, extensive experimental and numerical studies have been conducted to examine the seismic behaviour of steel columns, exploring various section types. This research has been significantly advanced by contributions from Newell and Uang (2006), Fogarty and S. El-Tawil (2016), Ozkula et al. (2017), Elkady and Lignos (2018b, 2018a), Cravero et al. (2020) and Suzuki and Lignos (2021), Ozkula and Uang (2023) among others.

Over the past two decades, various codes and guidelines have emerged for the seismic performance assessment of existing structures, including FEMA 356 (2000), AISC 342 (2022), and ASCE 41 (2023). Unlike design codes for new buildings, which primarily follow a force-based design philosophy, these

assessment codes generally adopt more contemporary seismic design approaches such as Performance-Based Design (PBD) and Displacement-Based Design (DBD). PBD and DBD focus on understanding the nonlinear behaviour of structural elements to evaluate the extent of damage, particularly in deformation-controlled components. To this end, numerous methodologies have been developed to estimate the deformation capacity of structural members under various internal forces. A prominent method is the Direct Rotation Method, which utilizes empirical formulas derived from experimental and numerical studies to predict the force-displacement relationships and ultimate deformation capacity of structural elements.

Alongside empirical methods, analytical approaches are also employed to estimate the force-displacement relationships of structural elements. The Plastic Hinge Analysis Method, a widely recognized technique, is instrumental in constructing moment-curvature and force-displacement curves for flexurally governed members, as evidenced by foundational works such as Blume et al. (1961) and Park and Paulay (1975). While this method has been extensively developed for reinforced concrete (RC) elements, its application to steel elements, particularly those susceptible to local buckling failure modes, has received comparatively less attention.

This study is one of the few that explores the Plastic Hinge Analysis Method as an analytical tool for estimating the force-displacement curve of steel columns predominantly failing due to local buckling. A FE parametric study is conducted to scrutinize the seismic behaviour of wide flange steel columns. Utilizing the outcomes of this numerical investigation, for the first time, an equivalent plastic hinge length is introduced specifically for wide flange steel columns, from which their displacement capacity can be determined. Subsequently, the accuracy of the Plastic Hinge Analysis Method, in conjunction with the proposed plastic hinge length approach is evaluated, by comparing it against test results from the existing literature.

2 RELATIONSHIP BETWEEN CURVATURE AND DISPLACEMENT

In the Plastic Hinge Analysis Method, the flexural plastic behaviour of an element is represented by an equivalent element, where plasticity is concentrated along an equivalent plastic hinge length (L_p), as depicted in Figure 1. To derive the force-displacement curve of a member using this method, the initial step involves calculating the moment-curvature relationship of the section via a section analysis procedure. This requires selecting suitable uniaxial stress-strain models for different materials of the section. Subsequently, the total displacement of the element at various limit states, related to the section curvature (ϕ_u), is determined. This is achieved by adding the yield displacement (Δ_y) to the plastic displacement (Δ_p), as delineated in the following equations for a double bending element:

$$\Delta_y = \frac{\phi_y l^2}{6} + \frac{2M_y}{GA_g} \quad (1)$$

$$\Delta_t = \Delta_y + (\phi_u - \phi_y)L_p(l - L_p) \quad (2)$$

Where, ϕ_y and M_y are the yield curvature and moment, respectively. l is the column height and A_g is its gross section area. Moreover, $G = \frac{E}{2(1+\nu)}$ is the shear modulus of material related to the elastic modulus (E) and Poisson ratio (ν). In Equation (2), the equivalent plastic hinge length (L_p) is a key parameter which is necessary for converting the section curvature to element's displacement.

The lateral load at different loading stages (F_i) corresponding to internal bending moment (M_i), and yield force (F_y) are calculated for a double bending element as follows:

$$F_y = \frac{2M_y}{l} \text{ (until yield)} \quad (3)$$

$$F_i = \frac{2M_i}{l-L_p} \text{ (after yield)} \quad (4)$$

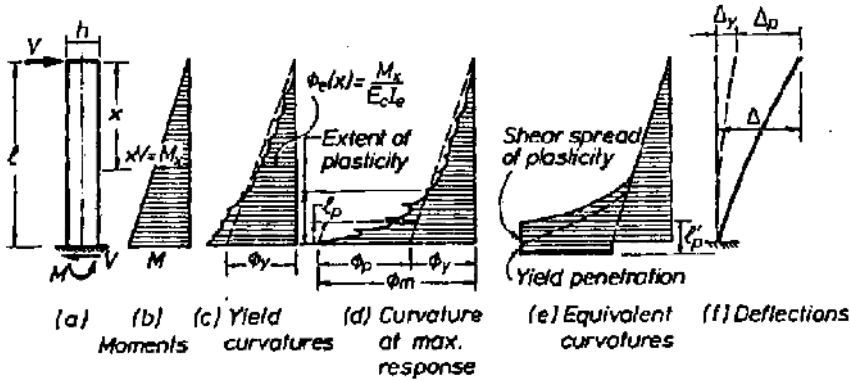


Figure 1. Moment, curvature, and deflection relationships for a RC cantilever element subjected to a point load (Paulay and Priestley 1992)

3 PLASTIC HINGE ANALYSIS OF STEEL COLUMNS

Unlike RC members, where well-established nonlinear material models exist for both concrete (Kent and Park 1971, Mander et al. 1988, Saatcioglu and Razvi 1992) and steel reinforcement (Menegotto and Pinto 1973), the development of equivalent plastic hinge lengths and suitable material models for steel members, especially those exhibiting local buckling behaviour, remains limited. This is despite the importance of both the equivalent plastic hinge length and the stress-strain model in effectively conducting plastic hinge analyses of such members.

3.1 Stress-strain material model for steel

In this research, a recently developed stress-strain model developed by Kolwankar et al. (2020) is employed for the plastic hinge analysis of steel columns. This model was derived from a detailed numerical study for wide flange steel columns subjected to cyclic loads as illustrated in Figure 2. A key feature of this model is its consideration of local buckling in steel columns with wide flange sections. Within this model, the stress and strain at the point of buckling, denoted as $\sigma_{y_{cap}}$ and $\varepsilon_{y_{cap}}$, respectively, are characterized as follows:

$$\sigma_{y_{cap}} = 1.1 \times \sigma_u - 2.17 \times (b_f/2t_f) \quad (5)$$

$$\varepsilon_{y_{cap}} = \frac{\sigma_y}{E} + \frac{\sigma_{y_{cap}} - \sigma_y}{h \times E} \quad (6)$$

Where, σ_y and σ_u are the steel yield and ultimate strength, $b_f/2t_f$ is the flange slenderness, and h is the strain hardening parameter which is assumed as 0.05 in this model suggested by Elkady and Lignos (2015).

The slopes of the softening branch of the stress-strain model in compression, $E_{d1.m}$ and $E_{d2.m}$, respectively, are determined as follows:

$$E_{d1.m} = (\sigma_{d_{cap}} - \sigma_{y_{cap}}) / \varepsilon_{res} \quad (7)$$

$$E_{d2.m} = 0.2 * E_{d1.m} \quad (8)$$

In these equations, the residual stress and strain, $\sigma_{d_{cap}}$ and ε_{res} can be determined by the following equations.

$$\sigma_{d_{cap}} = \sigma_y - 1.44 \frac{b_f}{2t_f} \geq 0 \quad (9)$$

$$\varepsilon_{res} = 0.15 - 0.014 \frac{b_f}{2t_f} \geq \frac{\sigma_y}{E} + \frac{\sigma_{cr} - \sigma_y}{h \times E} \quad (10)$$

In order to define the stress-strain behavior of steel in tension, some parameters related to kinematic and isotropic hardening including Q , b , c , and γ are needed. These parameters are determined by means of axial test for any types of steel.

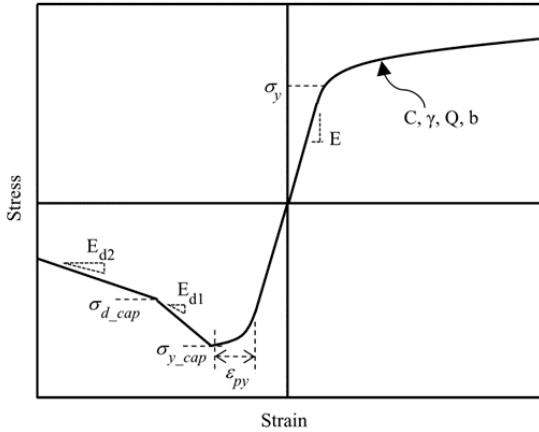


Figure 2. Stress-strain model for steel proposed by Kolwankar et al. (2020)

3.2 Available equivalent plastic hinge length models for steel column

Although the application of plastic hinge analysis in PBD and DBD for steel structures is not widespread in practice, three distinct formulations for calculating the plastic hinge length of steel columns have been proposed in the literature (Equations 11-13). It is important to note that some of these plastic hinge lengths referenced in literature represent the actual length over which plasticity develops in the elements, rather than the equivalent plastic hinge length typically used in plastic hinge analysis to determine an element's plastic displacement capacity. According to Bruneau et al. (2011) in Equation 11 and MacRae (1989) in Equation 12, the plastic hinge length is directly related to the height of the column (l) and the section depth (d), respectively. In contrast, Equation 12, proposed by Elkady and Lignos (2018b), defines the plastic hinge length as a function of the section web slenderness, the global slenderness of the column, and the axial load intensity.

$$LP_1 = 0.067L_c \quad (11)$$

$$LP_2 = 1.837d \left(\frac{h}{t_w}\right)^{-0.443} \left(\frac{L_b}{r_y}\right)^{0.287} \left(1 - \frac{P}{P_y}\right)^{-0.259} \quad (12)$$

$$LP_3 = d \quad (13)$$

Where, L_c is the length from the critical section to the point of contraflexure in the member, h/t_w is the web slenderness, L_b is the laterally unbraced length of the column, r_y is the weak-axis radius of gyration, P is the axial load, and P_y is axial yield strength.

3.3 Database of tests on wide flange steel columns

To evaluate the effectiveness of the plastic hinge analysis method in determining the force-displacement curve and drift capacity of steel columns, a database of 33 wide flange steel section specimens is compiled. These specimens, previously tested under cyclic lateral loads in experimental studies, predominantly failed due to local buckling. The characteristics of these test specimens are detailed in Table 1. Using the plastic

hinge analysis method, the lateral load-displacement curves for each column is analysed and their ultimate drift capacity is determined.

Table 1. A summary of the test specimens in the experimental database

Number	Tested by	Section	$b_f/2t_f$	h/t_w	L_b/r_y	P/P_y	Boundary conditions	
1	Ozkula et al. (2017)	W30x173	7.04	40.8	63.16	0.4	Fixed-fixed	
2		W30x173					Fixed-flexible	
3		W30x90	8.52	57.5	75	0.2	Fixed-fixed	
4		W24x176					Fixed-fixed	
5		W24x176	4.81	28.7	52	0.4	Fixed-fixed	
6		W24x176					Fixed-fixed	
7		W24x176	0.6	Fixed-flexible				
8		W24x131			Fixed-fixed			
9		W24x131	6.7	35.6	53	0.4	Fixed-fixed	
10		W24x131					Fixed-fixed	
11		W24x104	8.5	43.1	54	0.2	Fixed-fixed	
12		W24x104					Fixed-fixed	
13		W24x104	0.6	Fixed-fixed				
14		W24x84			Fixed-fixed			
15		W24x84	5.86	45.9	81	0.2	Fixed-fixed	
16		W18x130					Fixed-fixed	
17		W18x130	4.56	23.9	58	0.4	Fixed-flexible	
18		W18x76					Fixed-fixed	
19	Elkady and Lignos (2018a)	W24x146	5.92	33.2	52	0.2	Fixed-fixed	
20		W24x146					Fixed-flexible	
21		W24x84	5.86	45.9	81	0.2	Fixed-flexible	
22	Cravero et al. (2020)	W14x82	5.92	22.2	64	0.5	Fixed-flexible	
23		W14x82					0.75	Fixed-flexible
24		W16x89	5.92	27	63	0.5	Fixed-flexible	
25	Suzuki et al. (2021)	W14x53	6.11	30.9	82	0.3	Fixed-flexible	
26		W14x61	7.75	30.4	64	0.3	Fixed-flexible	
27		W14x82	5.92	22.4	64	0.3	Fixed-flexible	
28	MacRae (1989)	C3	8.94	37.6	78.57	0.3	Fixed-flexible	
29		C4					0.4	Fixed-flexible
30		C5					0.5	Fixed-flexible
31		C6					0.6	Fixed-flexible
32		C7	0.7	Fixed-flexible				
33		C8	0.8	Fixed-flexible				

The mean, standard deviation, and coefficient of variation for the estimated versus experimental drift capacities of the columns, using different equivalent plastic hinge length equations, were determined, and presented in Table 2. A mean value exceeding one indicates an overestimation of the column's drift capacity by the model. The findings reveal that using the existing plastic hinge lengths (Equations 11-13) by means of the plastic hinge analysis method does not yield sufficiently accurate results. Therefore, to enhance the method's accuracy in estimating the drift capacity of columns, the development of a more appropriate equivalent plastic hinge length is essential.

Table 2. Evaluation of the analytical drift vs experimental results

Method	Analytical/Experimental drift estimation		
	Mean	Standard Deviation	COV
LP_1 (Bruneau et al. 2011)	0.72	0.33	0.46
LP_2 (Elkady and Lignos 2018b)	1.79	0.79	0.44
LP_3 (MacRae 1989)	1.43	0.59	0.41

4 FINITE ELEMENT ANALYSIS OF COLUMNS

To identify a suitable plastic hinge length for steel columns with wide flange sections, a numerical study is conducted using the FE software Abaqus. The main reason for using numerical results was lack of sufficient experimental data for developing an empirical equation. Initially, the FE model was validated against test results from steel columns carried out in previous studies. Following this validation, a comprehensive parametric study was undertaken, leading to the proposal of a new expression for the equivalent plastic hinge length of steel columns.

4.1 Validation of the FE model

4.1.1. The test specimens

The FE model was validated against several columns experimentally tested by other researchers. For the sake of brevity in this paper, the results from only three representative columns are presented. These selected columns, varying in section sizes and axial load levels, were part of the series tested by Ozcuca et al. (2017). Detailed information about the test specimens and the mechanical properties of the steel used (ASTM A992-Gr.50), determined through standard tensile tests in the experimental program, are provided in Table 3.

Table 3. The details of the test specimens simulated in the present study

Section	Yield Stress (Mpa)		Tensile Stress (Mpa)		Modulus of Elasticity (Mpa)	Lateral Loading Protocol	p/p_y	$b_f/2t_f$	h/t_w	L_b/r_y
	Flange	Web	Flange	Web						
W24x131	350	382	523	536	200000	AISC-Symmetric Loading Protocol	0.4	6.7	35.6	72.7
W24x104	355	401	538	556	200000		0.2	8.5	43.1	40.6
W24x84	350	382	523	536	200000		0.2	5.86	45.9	110.8

4.1.2. Details of the FE modelling

The analysis of columns was performed using 4-node double-curvature shell elements (S4R) with a maximum mesh size of 25 mm, as illustrated in Figure 3. The S4R element in the FE software Abaqus is capable of simulating large, three-dimensional nonlinear deformations. Initial imperfections are incorporated into the element and the model, based on the recommendations provided by Elkady and Lignos (2018b). The steel's nonlinear stress-strain behaviour was simulated using a bilinear elasto-plastic stress-strain model. To

capture the steel's nonlinear response under cyclic loads, the Von Mises yield criterion and a combined hardening rule were employed. This model requires defining specific parameters, including Q , b , and γ . In this study, the values of these parameters ($Q=90$ MPa, $b=12$, $\gamma=20$, and $C=3378$ MPa) were chosen based on the recommendations for ASTM A992-Gr.50 steel material by Elkady and Lignos (2018b). To simulate the top and bottom fixed boundary conditions of the columns, the degrees of freedom at the nodes located at both ends were restrained, as depicted in Figure 3. For the specimens subjected to constant axial load in testing, the axial and lateral loads were applied to the model in two distinct steps. Initially, an axial load, matching the magnitude reported in the experimental tests, was applied to the column. Subsequently, this axial load was maintained constant, and a cyclic displacement-controlled load was applied to the column's top, following the same loading protocol as in the experimental tests.

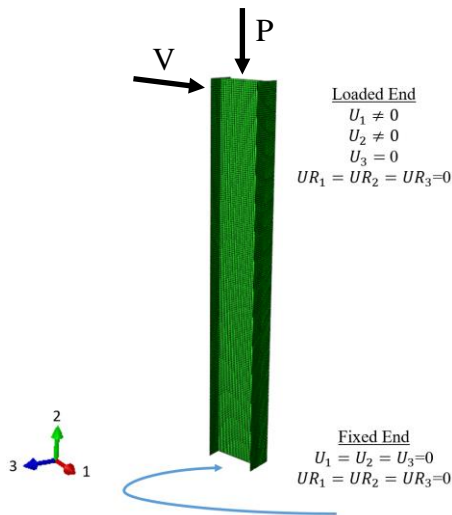


Figure 3. The geometry of the test specimens made in FE software Abaqus and the generated shell elements

4.1.3. Analysis results

The hysteresis moment-drift curves for the three columns, both experimental and numerical, are compared in Figure 4. The numerical curves closely align with the results from the experimental tests, demonstrating a very good agreement. Additionally, Table 4 shows the ultimate failure modes of the columns. As indicated, the FE model successfully replicated the primary failure mode of the columns, which was predominantly local buckling.

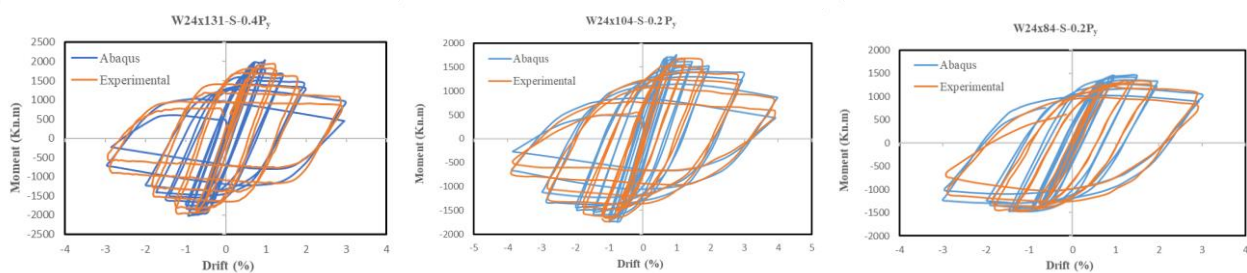

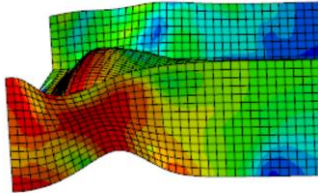

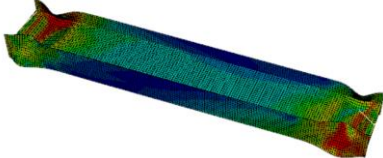

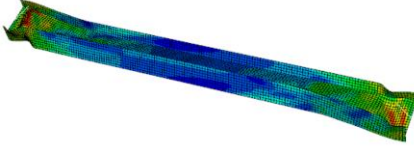


Figure 4. Experimental vs numerical hysteresis moment-drift curves of the columns tested by Ozcula et al. (2017)

Table 4. The comparison of the ultimate failure mode of the columns obtained from the tests and numerical studies

Specimen	Failure mode (test)	Failure mode (Numerical Study)	Comparison drift
W24x131-S-0.4Py			4.0%
W24x104-S-0.2Py			4.0%
W24x84(4L)			3.0%

4.2 Parametric study

To assess the impact of various factors, such as the geometrical properties of the columns and the intensity of axial loads, on the seismic behaviour of steel columns with wide flange sections, a comprehensive parametric study was undertaken using the validated FE model. This study involved analysing columns with 20 different wide flange sections under five levels of constant axial loads (10%, 20%, 35%, 50%, and 60%), encompassing a broad spectrum from low to high axial load intensities typically observed in steel frames. Consequently, a total of 100 columns, all with fixed-restrained boundary conditions at both ends, were simulated and analysed. The chosen wide flange sections featured flange slenderness ratios in the range of $3.1 < b_f/2t_f < 8.52$ and web slenderness ratios of $6.9 < h/t_w < 57.5$. The global slenderness ratios of these columns varied between $36.9 < L_b/r_y < 117.5$. All columns in the parametric study were modelled with an identical height of 4.0 meters.

5 DEVELOPING AN EQUIVALENT PLASTIC HINGE FOR STEEL COLUMNS

An expression for the equivalent plastic hinge length of steel columns with wide flange sections is proposed. Utilizing a database from our numerical study, the required plastic hinge length to accurately capture the drift capacity was determined for each column. The drift capacity criterion was defined as a 20% reduction in strength on the force-displacement curve, indicative of local buckling failure mode. Since plastic hinge length is associated with local behaviour of columns, the database was confined to models exhibiting local buckling failure modes, encompassing 60 models. Columns exhibiting lateral torsional buckling failure were consequently excluded. The efficacy of the plastic hinge analysis method, in conjunction with our proposed plastic hinge length, was validated by comparing our analytical results with experimental test data. The final

expression for the plastic hinge length emerged from a nonlinear regression analysis, achieving a correlation coefficient $R^2 = 0.77$ as follows:

$$L_{p,proposed} = 13.192d \left(\frac{P}{P_y}\right)^{-0.653} \left(\frac{b_f}{2t_f}\right)^{1.617} \left(\frac{h}{t_w}\right)^{-1.276} \left(\frac{l}{r_y}\right)^{-0.481} \quad (14)$$

The estimated drift capacities of the columns are compared with the results from FE analyses in Figure 5. The mean and standard deviation of the ratio of estimated drift to FE-analysed drift for the columns are 1.04 and 0.18, respectively, resulting in a coefficient of variation (COV) of 0.17. This indicates that the method not only accurately estimates the drift capacity of columns but also yields results with relatively low variability.

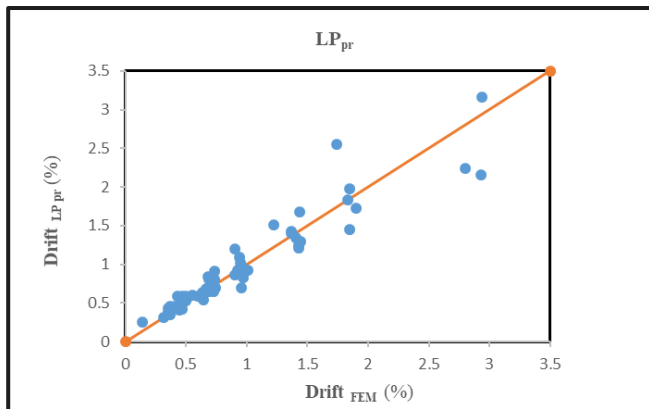


Figure 5. The estimated vs. actual lateral drift capacity of the columns investigated in numerical study

6 CONCLUSIONS

This study involved a comprehensive numerical investigation, using a validated FE model, to explore the seismic behaviour of steel columns with wide flange sections. A pivotal aspect of this research was the first-time assessment of the plastic hinge analysis method's effectiveness in estimating the force-displacement behaviour of steel columns exhibiting a local buckling failure mode. Central to this investigation was the development of a new expression for the equivalent plastic hinge length of steel columns, derived from an extensive numerical parametric study. Upon comparing the outcomes of analytical calculations with experimental data, it was demonstrated that the plastic hinge analysis method, complemented by the proposed plastic hinge length, accurately predicts the ultimate drift capacity of steel columns. This finding underscores the method's validity and potential applicability in seismic analysis of steel structures.

REFERENCES

- AISC342-22 (2022). Seismic Provisions for Evaluation and Retrofit of Existing Structural Steel Buildings (ANSI/AISC 342), AISC Chicago, IL.
- ASCE41-23 (2023). Seismic Evaluation and Retrofit of Existing Buildings, American Society of Civil Engineers, Reston, Virginia.
- Blume, J. A., N. M. Newmark and L. H. Corning (1961). Design of multistory reinforced concrete buildings for earthquake motions, Portland Cement Association Chicago.
- Bruneau, M., C.-M. Uang and S. R. Sabelli (2011). Ductile design of steel structures, McGraw Hill Professional.
- Cravero, J., A. Elkady and D. G. Lignos (2020). "Experimental evaluation and numerical modeling of wide-flange steel columns subjected to constant and variable axial load coupled with lateral drift demands." Journal of Structural Engineering **146**(3): 04019222.

- Elkady, A. and D. G. Lignos (2015). "Analytical investigation of the cyclic behavior and plastic hinge formation in deep wide-flange steel beam-columns." Bulletin of Earthquake Engineering **13**: 1097-1118.
- Elkady, A. and D. G. Lignos (2018a). "Full-scale testing of deep wide-flange steel columns under multiaxis cyclic loading: Loading sequence, boundary effects, and lateral stability bracing force demands." Journal of Structural Engineering **144**(2): 04017189.
- Elkady, A. and D. G. Lignos (2018b). "Improved seismic design and nonlinear modeling recommendations for wide-flange steel columns." Journal of Structural Engineering **144**(9): 04018162.
- FEMA 356, F. E. (2000). "Prestandard and commentary for the seismic rehabilitation of buildings." Federal Emergency Management Agency: Washington, DC, USA.
- Fogarty, J. and S. El-Tawil (2016). "Collapse resistance of steel columns under combined axial and lateral loading." Journal of Structural Engineering **142**(1): 04015091.
- Kent, D. C. and R. Park (1971). "Flexural members with confined concrete." Journal of the structural division **97**(7): 1969-1990.
- Kolwankar, S., A. Kanvinde, M. Kenawy, D. Lignos and S. Kunnath (2020). "Simulating Cyclic Local Buckling-Induced Softening in Steel Beam-Columns Using a Nonlocal Material Model in Displacement-Based Fiber Elements." Journal of Structural Engineering **146**(1): 04019174.
- MacRae, G. A. (1989). The seismic response of steel frames. Ph.D. thesis, University of Canterbury, Christchurch, New Zealand.
- Mander, J. B., M. J. N. Priestley and R. Park (1988). "Theoretical stress-strain model for confined concrete." Journal of structural engineering **114**(8): 1804-1826.
- Menegotto, M. and P. E. Pinto (1973). "Method of analysis for cyclically loaded reinforced concrete frames including changes in geometry and non-elastic behavior of elements under combined normal forces and bending moment." IASBE Proceedings.
- Newell, J. D. and C.-M. Uang (2006). Cyclic behavior of steel columns with combined high axial load and drift demand, Department of Structural Engineering, University of California, San Diego.
- Ozkula, G., J. Harris and C.-M. Uang (2017). "Observations from cyclic tests on deep, wide-flange beam-columns." Engineering Journal **54**: 45-60.
- Ozkula, G. and C.-M. Uang (2023). "Classification and Identification of Buckling Modes of Steel Columns under Cyclic Loading." Journal of Structural Engineering **149**(8): 04023097.
- Park, R. and T. Paulay (1975). Reinforced concrete structures, John Wiley & Sons.
- Paulay, T. and M. J. N. Priestley (1992). seismic design of reinforced concrete and masonry buildings. New York, USA, John Wiley & Sons, Inc.
- Saatcioglu, M. and S. R. Razvi (1992). "Strength and ductility of confined concrete." Journal of Structural engineering **118**(6): 1590-1607.
- SAP2000 Version 21.0.2 (2019). Integrated Finite Element Analysis and Design of Structures. Computers and Structures Inc, Berkeley, California, USA.
- Suzuki, Y. and D. G. Lignos (2021). "Experimental evaluation of steel columns under seismic hazard-consistent collapse loading protocols." Journal of Structural Engineering **147**(4): 04021020.